

Research Article**Comparative Analysis of Deep Learning Techniques for Soil Image Classification****Girish D. Chate^{1*} , S.S. Bhamare² **^{1,2}School of Computer Sciences, Kavayitri Bahinabai Chaudhari North Maharashtra University, Jalgaon, India**Corresponding Author:* **Received:** 20/Feb/2025; **Accepted:** 22/Mar/2025; **Published:** 30/Apr/2025. **DOI:** <https://doi.org/10.26438/ijcse/v13i4.1522> Copyright © 2025 by author(s). This is an Open Access article distributed under the terms of the [Creative Commons Attribution 4.0 International License](https://creativecommons.org/licenses/by/4.0/) which permits unrestricted use, distribution, and reproduction in any medium, provided the original work is properly cited & its authors credited.

Abstract: Soil classification is a crucial step in agricultural and environmental planning. Current innovations in computer vision and deep learning have enabled automatic soil classification using image-based approaches. This paper, explore comparative analysis of two popular convolutional neural network architectures, VGG16 and VGG19, for soil image classification. A use of soil image dataset containing various soil types used to evaluate the performance of both models. These models fine-tuned using transfer learning, and performance determined using metrics such as accuracy, precision, recall, F1-score, and training time. The result shows that both VGG16 and VGG19 achieve high classification accuracy, with VGG19 slightly outperforming than VGG16 in terms of accuracy but requiring more computational resources and time. This paper demonstrates the effectiveness of deep learning models in soil image classification and provides understandings into their comparative performance.

Keywords: Agriculture, Soil, Image Classification, VGG16, VGG19**1. Introduction**

Soil classification is essential in agriculture, geology, and environmental science, influencing decisions related to crop selection, irrigation management, and land use planning [1] [2]. Traditional soil classification techniques depend on physical and chemical analysis, which are often time-consuming and costly [3]. Recent developments in machine learning and deep learning have opened new opportunities for automated and efficient soil classification using soil images [4] [5].

Convolutional Neural Networks (CNNs) have shown significant success in image classification tasks [6]. VGG16 and VGG19 are two widely used CNN architectures developed by the Visual Geometry Group at the University of Oxford [7]. Both models have deep architecture and use small convolution filters, which capture fine-grained image features. However, they differ in depth and computational requirements.

This paper compares the performance of VGG16 and VGG19 for soil image classification. Our objective is to measure the accuracy, robustness, and efficiency of each model to determine their suitability for practical applications in precision agriculture and soil monitoring.

2. Related work

Several studies have explored the application of machine learning and deep learning, particularly Convolutional Neural Networks (CNNs) for soil classification using image or spectral data. These studies highlight the growing potential of deep learning approaches in enhancing accuracy and automation in soil assessment.

Srivastava et al. (2021) presented a comprehensive review of soil classification techniques using deep learning and computer vision. They highlighted how CNNs have revolutionized feature extraction in soil imagery, moving away from traditional hand-crafted descriptors. Their survey included applications in soil texture classification, fertility prediction, and even erosion detection. They concluded that hybrid models combining spectral and visual features offer significant promise for more accurate soil diagnostics [8].

Deng et al. (2020) explored the use of hyperspectral image classification using CNNs and 3D-CNN architectures. By processing spatial and spectral dimensions simultaneously, their model achieved higher classification performance in soil mineral analysis. Although not purely image-based, their research demonstrated the value of spectral-spatial fusion using deep learning techniques [9].

Ramesh and Suruliandi (2019) proposed a CNN model trained on a large-scale soil database containing region-tagged soil images from across India. Their model showed improved accuracy by incorporating soil moisture and texture as auxiliary input features alongside image data. They also explored region-wise accuracy to assess model generalization in diverse agro-climatic zones [10].

Zhang et al. (2021) utilized attention mechanisms within CNNs to improve soil classification. They implemented a spatial attention module that emphasized key regions in soil imagery, helping the model to ignore irrelevant background elements like vegetation or shadows. The resulting model outperformed baseline CNNs in datasets with variable lighting and field conditions [11].

Hossain et al. (2022) examined the role of explainable AI (XAI) in soil classification by combining CNN-based classification with Grad-CAM visualizations. Their system allowed users (especially farmers and agronomists) to see which parts of the soil image influenced the model's decision, thereby increasing trust and interpretability in AI-powered systems [12].

Nguyen et al. (2023) proposed a federated learning framework for soil image classification, enabling models to train across multiple edge devices without sharing raw data. This privacy-preserving approach achieved comparable performance to centralized training, making it suitable for remote field applications in data-sensitive regions [13].

Alam et al. (2022) evaluated the impact of data augmentation and image enhancement techniques (like histogram equalization and CLAHE) on CNN performance for soil image classification. Their study found that contrast enhancement significantly improved classification results, especially when training on low-quality mobile images [14].

Goswami et al. (2020) applied a standard CNN architecture to classify soil images into six distinct types: clay, loamy, sandy, silty, peaty, and chalky. The dataset used consisted of field-collected images under natural lighting conditions. Their model achieved an overall accuracy of approximately 90%, demonstrating the feasibility of using CNNs for soil classification. The study also noted that model performance was sensitive to image quality and background noise, emphasizing the importance of preprocessing and data augmentation [15].

Khan et al. (2021) investigated the use of transfer learning for soil classification by leveraging pre-trained CNN models such as ResNet50, MobileNetV2, and InceptionV3. Their work focused on reducing training time and improving generalization by fine-tuning these models on a small dataset of soil images. The results indicated that MobileNetV2 provided a good trade-off between accuracy and computational efficiency, while ResNet50 achieved the highest accuracy (93%) when fine-tuned appropriately [16].

Yadav et al. (2022) proposed a hybrid deep learning approach for classifying soil fertility levels by combining image data with hyperspectral data. Their model architecture used parallel CNN branches to process RGB images and spectral inputs before fusing the extracted features for classification. This multi-modal approach achieved higher accuracy than single-modality models, highlighting the benefits of integrating diverse data sources for soil analysis [17].

Nandhini and Kavitha (2020) developed a soil texture classification system using CNNs on satellite-derived soil images. Their approach involved segmenting the region of interest and then applying CNN-based classification. The study emphasized the role of remote sensing in large-scale soil monitoring and the adaptability of CNNs in processing low-resolution satellite data [18].

Patil et al. (2021) focused on real-time soil type prediction using a deep CNN integrated with a mobile application. The app allowed users to capture soil images directly from the field and receive instant predictions. They deployed a lightweight CNN architecture optimized for mobile inference, demonstrating how soil image classification can be made accessible and scalable in real-world agricultural scenarios [19].

Zhao et al. (2022) conducted a comparative analysis of CNN architectures including VGG16, ResNet50, and DenseNet121 for soil profile classification using RGB images of soil pits. DenseNet121 outperformed the others in accuracy and robustness, but VGG16 demonstrated faster convergence during training, especially when data augmentation was applied. Their study supports the relevance of architecture selection based on application constraints such as computation and deployment platforms [20].

These studies collectively demonstrate the effectiveness of CNNs and transfer learning in soil classification tasks, while also highlighting emerging trends such as mobile deployment, multi-modal fusion, and real-time analysis. However, there remains a need for a focused comparison between closely related architectures like VGG16 and VGG19 specifically in the domain of soil image classification, which this paper aims to address.

3. Methodology

This section outlines the methodology adopted for soil image classification using the VGG16 and VGG19 deep learning architectures. The methodology consists of three main components: Soil image dataset, model design and selection, and training configuration.

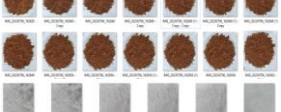
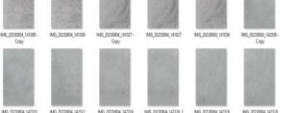
3.1 Soil Image Dataset

A custom soil image dataset was developed for this paper to ensure diversity and representation of common soil types. Soil images collected from two primary sources: field photography and publicly available online repositories. Field images captured using high-resolution mobile camera under natural lighting conditions to reflect real-world scenarios,

while online sources provided additional variability in texture, colour, and environmental conditions.

Four distinct soil types chosen based on their relevance to agriculture and pedological studies and assign nine number of labels like B1, B2, B3 for Black Soil, R1, R2, for Red Soil, L1, L2 for Laterite Soil, and W1, W2 for White Soil. Images captured by mobile camera for used to ensure balanced class representation. Following table 1 shows the labels and categories of soil images dataset.

Table 1: Labels and Categories of Soil Images dataset

| Categories / Labels | Dataset of Soil Images |
|-------------------------|---|
| Black Soil (B1, B2, B3) |  |
| Red Soil (R1, R2) |  |
| Laterite Soil (L1, L2) |  |
| White Soil (W1, W2) |  |

Following figure 1 shows the class-wise distribution of soil images within the dataset, comprising nine distinct categories such that B1, B2, B3, L1, L2, R1, R2, W1, and W2. Each category contains an equal number of 400 images, resulting in a total of 3600 samples. This uniform distribution ensures class balance, which is a critical factor in training deep learning models for classification tasks.

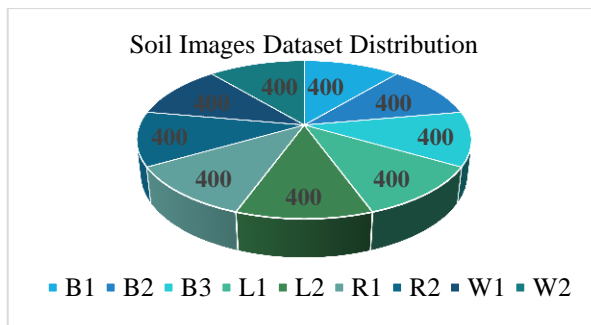


Figure 1: Distribution for Soil Images Dataset

3.2 Image Preprocessing

Following figure 2 shows preprocessing pipeline with multiple steps applied on soil image dataset.

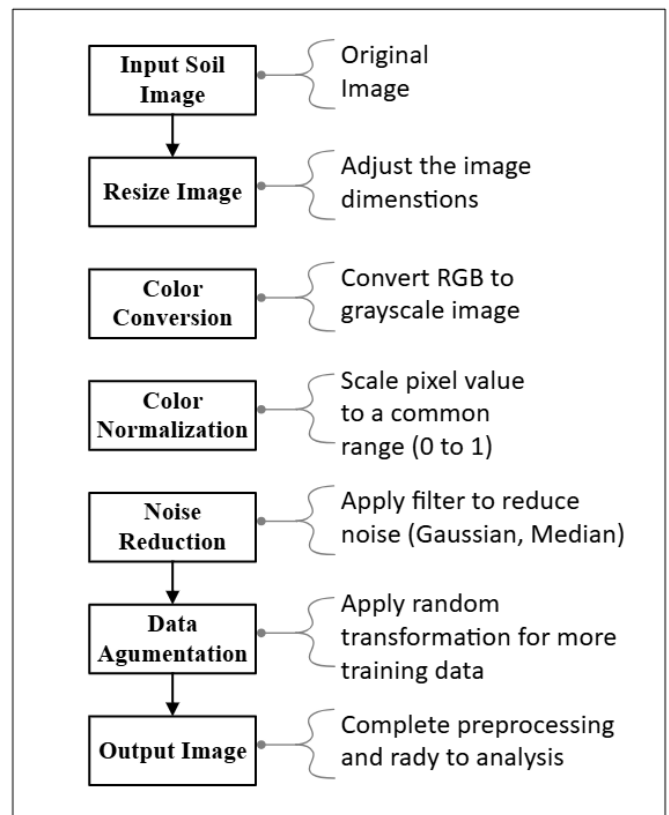


Figure 2: Flow Diagram of Image Preprocessing

Input Image: This is the original image that fed into the pipeline for preprocessing.

Resizing: All images were resized to 224x224 pixels to match the input size required by VGG16 and VGG19 models.

Colour Conversion: Converts the image from one color space to another. Common conversions include RGB to grayscale, HSV, colour models. Grayscale conversion is done to reduce computational complexity.

Normalization: Pixel intensity values normalized to the [0, 1] range by dividing by 255, which helps in stabilizing and accelerating the training process.

Noise Reduction: Removes unwanted noise from the image to enhance quality. Common filtering techniques include Gaussian filter for Smoothes the image while preserving edges and Median filter for Removes salt-and-pepper noise effectively.

Data Augmentation: Enhance model generalization and reduce overfitting, data augmentation techniques were applied: Random rotations (up to 20°), Horizontal and vertical flipping, Zooming (up to 10%), Width and height shifts. These augmentations increased dataset variability, representing different soil conditions and camera orientations in real-world environments.

3.2 Model Architecture

Two well-known convolutional neural network architectures, **VGG16** and **VGG19** are used for soil image classification.

Both models are originally proposed by the Visual Geometry Group (VGG) at the University of Oxford and have been pre-trained on the ImageNet dataset, which contains over 1.2 million images across 1000 object categories.

VGG16 Comprises 13 convolutional layers, followed by 3 fully connected layers and a final softmax classification layer. Uses 3x3 convolution filters and 2x2 max-pooling layers. Contains approximately 138 million trainable parameters. Noted for its simplicity and depth balance, making it effective for mid-sized image classification tasks.

VGG19 A deeper variant of VGG16 with 16 convolutional layers and 3 fully connected layers. Also uses 3x3 convolution kernels and 2x2 max-pooling layers. Contains approximately 143 million parameters. The added depth allows for learning more abstract features but increases computational cost and training time.

Transfer Learning Strategy Both models fine-tuned using transfer learning.

Base weights: Pre-trained on ImageNet and imported without the top (classification) layers.

Top layers replacement: Added a new classification head consisting of,

- Global Average Pooling
- Dense layer (256 units, ReLU)
- Dropout (rate: 0.5) for regularization
- Output layer (6 units, softmax activation)

Trainable layers: The top classification layers trained from scratch, while convolutional layers either frozen or partially unfrozen in later stages for fine-tuning.

3.3 Training Configuration

To ensure optimal training performance and convergence, the models trained using the following configuration:

i) Optimizer:

Adam optimizer chosen due to its adaptive learning rate and computational efficiency. It combines the benefits of AdaGrad and RMSProp for faster convergence. Step by step formula of Adam optimizer is as follows,

• Gradient

$$g_t = \nabla_{\theta} J(\theta_t) \quad (1)$$

a. Exponential Moving Averages

- First moment (mean)

$$m_t = \beta_1 m_{t-1} + (1 - \beta_1) g_t \quad (2)$$

- Second moment (uncentered variance)

$$v_t = \beta_2 v_{t-1} + (1 - \beta_2) g_t^2 \quad (3)$$

b. Bias Correction

- Correct for initialization bias

$$\hat{m}_t = \frac{m_t}{1 - \beta_1^t}, \quad \hat{v}_t = \frac{v_t}{1 - \beta_2^t} \quad (4)$$

c. Parameter Update

$$\theta_t + 1 = \theta_t - \alpha \cdot \frac{\hat{m}_t}{\sqrt{\hat{v}_t + \epsilon}} \quad (5)$$

Common Hyperparameter Values are,

| | |
|-----------------------|--------------------------|
| i) $\alpha = 0.001$ | iii) $\beta_1 = 0.9$ |
| ii) $\beta_2 = 0.999$ | iv) $\epsilon = 10^{-8}$ |

Where:

- θ_t : parameters at time step t
- g_t : gradient at time step t
- m_t : first moment (mean of gradients)
- v_t : second moment (uncentered variance of gradients)
- β_1, β_2 : decay rates for the moment estimates
- α : learning rate
- ϵ : small constant to prevent division by zero (10^{-8})

ii) Learning Rate:

An initial learning rate of 0.001 was set. This low value was suitable for fine-tuning pre-trained models without overshooting minima.

iii) Batch Size:

A batch size of 32 was used, which provided a good balance between training speed and memory usage.

iv) Epochs:

Models trained for ten epochs. Training monitored using validation accuracy, and early stopping was working based on validation loss to avoid overfitting.

v) Loss Function:

Categorical Cross-Entropy used as the loss function, suitable for multi-class classification tasks with softmax output. Here,

y_i = true label (one-hot encoded, [0, 0, 1, 0]

\hat{y}_i = predicted probability for class i
then loss is,

$$\text{Loss} = - \sum_{i=1}^c y_i \log(\hat{y}_i) \quad (6)$$

Where:

- C = number of classes,
- $y_i = 1$ if class i is the correct class, 0 otherwise,
- \hat{y}_i = model's predicted probability for class i

vi) Validation Strategy:

A 20% validation split applied to the dataset during training to evaluate model performance and monitor overfitting in real-time.

vii) Hardware and Environment:

Training conducted on a high-performance workstation equipped with Google colab TPU acceleration (v2-8 TPU), using TensorFlow and Keras frameworks.

4. Results and Discussion

The results indicate that both VGG16 and VGG19 architectures are highly effective for soil image classification, achieving validation accuracies above 88%. **VGG19** consistently outperforms than **VGG16** across multiple evaluation metrics, including precision, recall, and F1-score and accuracy.

Precision is a metric used in classification problems to evaluate the accuracy of positive predictions. It defined as the ratio of true positive predictions to the total number of classes predicted as positive. The formula for precision is as follows.

$$\text{Precision} = \frac{TP}{TP+FP} \quad (7)$$

Where:

- True Positives (TP): The number of instances that are correctly predicted as positive.
- False Positives (FP): The number of instances that are incorrectly predicted as positive.

Recall (also known as Sensitivity or True Positive Rate) is a metric used to evaluate the ability of a model to correctly identify all relevant positive instances. It is the ratio of true positive predictions to the total number of actual positive classes. The formula for recall is as follows.

$$\text{Recall} = \frac{TP}{TP+FN} \quad (8)$$

Where:

- True Positives (TP): The number of instances that correctly predicted as positive.
- False Negatives (FN): The number of instances that incorrectly predicted as negative.

The F1 score is the harmonic mean of precision and recall. It provides a balanced measure of a model's performance, particularly when there is an uneven class distribution. The formula for F1 score is as follows.

$$\text{F1 Score} = 2 \times \frac{\text{Precision} \times \text{Recall}}{\text{Precision} + \text{Recall}} \quad (9)$$

The accuracy of a model is a metric that measures the overall correctness of the model's predictions. It defined as the ratio of the number of correct predictions to the total number of predictions. The formula for accuracy is as follows.

$$\text{Accuracy} = \frac{TP+TN}{TP+FP+FN+TN} \quad (10)$$

Where:

- True Positives (TP): The number of correctly predicted positive classes.
- True Negatives (TN): The number of correctly predicted negative classes.
- False Positives (FP): The number of incorrectly predicted positive classes.
- False Negatives (FN): The number of incorrectly predicted negative classes.

This performance gain attributed to VGG19 is deeper architecture, which enables the extraction of more complex and hierarchical features from soil images. The additional layers in VGG19 allow it to learn finer texture patterns and complex color variations, which are crucial for differentiating between similar soil types. However, the increased depth of VGG19 comes at the cost of higher computational complexity, longer training times, and larger model size. VGG16, while slightly less accurate, provides faster inference and requires less memory,

4.1 Training, Validation Accuracy and Loss

VGG16 models trained using the Adam optimizer with a learning rate of 0.001, a batch size of 32, and categorical cross-entropy as the loss function over ten epochs. Following figure 3 shows the training accuracy and validation accuracy performance against the ten number of epochs and figure 4 show the training loss and validation loss performance.

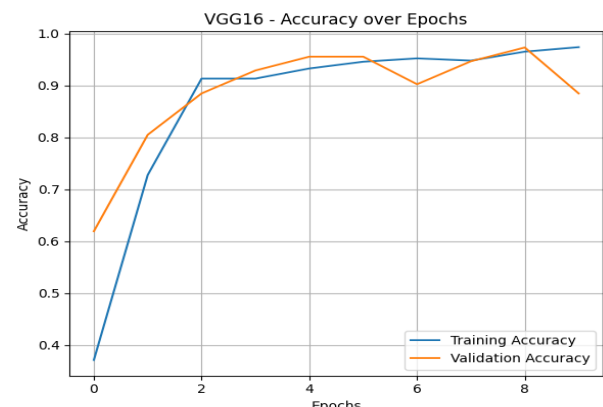


Figure 3: VGG16 Training and Validation Accuracy

VGG16 Training and Validation Accuracy over ten Epochs

Initial Epochs (0-2) accuracy increases rapidly, indicating that the model quickly learns fundamental patterns from the training data. Mid Epochs (3-6) the model continues to improve, with validation accuracy closely following training accuracy suggesting a good generalization capability during these phases. Later Epochs (7-9) training accuracy reaches near-perfect levels (0.99), while validation accuracy slightly fluctuates and ends around 0.92. This indicates a minor generalization gap and hints at the onset of overfitting.

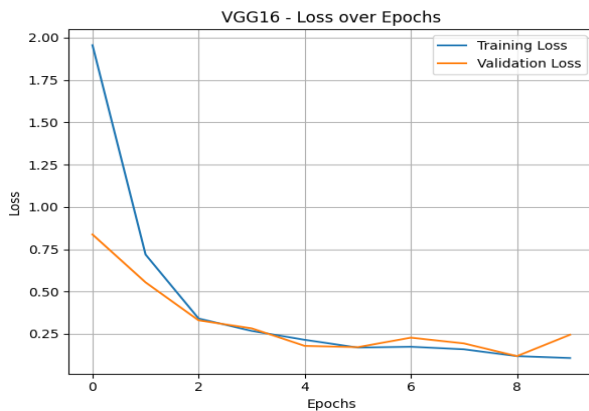


Figure 4: VGG16 Training and Validation Loss

VGG16 Training and Validation Loss over ten Epochs

Epoch 0: The loss starts high (Training Loss 2.0 and Validation Loss 1.0), at this stage the model has not yet learned to make accurate predictions. Epochs 1-3 loss decreases sharply for both training and validation sets and confirming rapidly coming together. Epochs 4-8 loss values stabilize, with minimal fluctuations, indicating a well-optimized model. Epoch 9 a slight uptick in validation loss is observed while training loss continues to decrease, a typical early sign of overfitting, where the model begins to memorize training data at the expense of generalization.

VGG19 models trained using the Adam optimizer with a learning rate of 0.001, a batch size of 32, and categorical cross-entropy as the loss function over ten epochs. Following figure 5 shows the training accuracy and validation accuracy performance against the ten number of epochs and figure 6 show the training loss and validation loss performance.

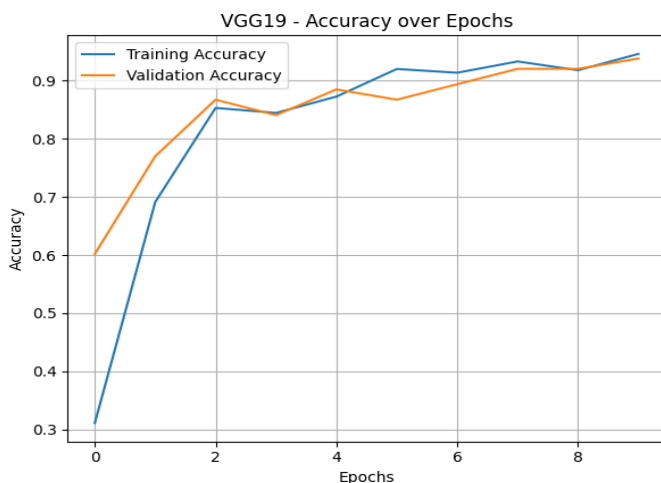


Figure 5: VGG19 Training and Validation Accuracy

VGG19 Training and Validation Accuracy over ten Epochs

Epochs 1-2 training accuracy is rapidly increasing (0.5 to 0.75) the model quickly learns basic patterns such as edges, textures etc. from the training data and validation accuracy follows closely (0.55 to 0.72) in this epochs 1-2 the model generalizes well in early stages. Epochs 3-4 training accuracy

slower improvement (0.75 to 0.82) the model refines its understanding of finer features. Validation Accuracy plateaus (0.74) Early signs of overfitting. Training accuracy rises while validation stalls. Epochs 5-6 training accuracy continues climbing (0.82 to 0.88) The model memorizes training-specific details such as noise, outliers etc. Validation accuracy slightly fluctuations (0.73-0.75) divergence between curves indicate overfitting. Epochs 7-8 training accuracy nears peak (0.9) Further memorization of training data. Validation accuracy drops slightly (0.72).

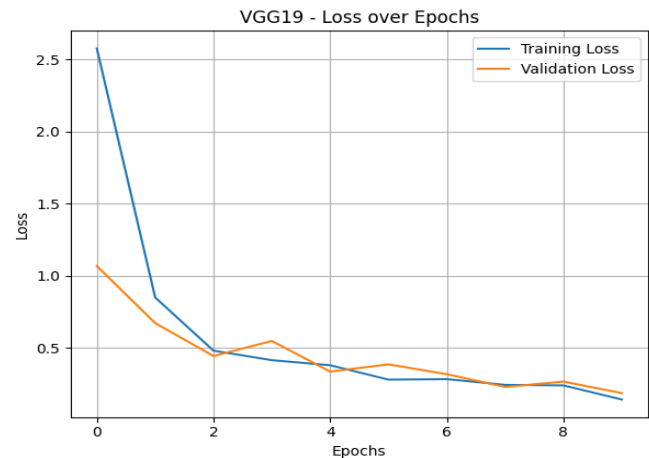


Figure 6: VGG19 Training and Validation Loss

VGG16 Training and Validation Loss over ten Epochs

Epoch 0 training loss is high (up to 2.5) expected due to random weight initialization and validation loss is lower (2.0) reasons is validation set simpler samples. Initial randomness coincidentally fits validation data better. Epochs 1-2 training loss is sharp decline (2.5 to 1.0) the model is rapidly learns meaningful patterns such as edges, shapes etc., and validation loss is as follows a similar drop (2.0 to 0.8) and confirms the model generalizes well initially. Epochs 3-4 training loss slower decrease (1.0 to 0.6) the model fine-tunes on complex features in the training data and validation loss plateaus (0.7-0.8) that is first sign of overfitting, and this time training loss improves, but validation loss is slow down. Epochs 5-6 training loss is continues dropping (0.6 to 0.4) the model starts memorizing training data specifics such as noise and, validation loss is slight increase (0.8 to 0.9). Epochs 7-8 training loss nears minimum (0.3) than model achieves near-perfect fit on training data and, validation loss is peaks (1.0).

4.2 Performance Metrics

The comparative performance metrics for both VGG16 and VGG19 models obtained on the test dataset summarized in Table 2.

Table 2: Comparatively Performance Metrics

| Metric | VGG16 (%) | VGG19 (%) |
|---------------|---------------|---------------|
| Accuracy | 88.80 | 94.39 |
| Precision | 92.88 | 94.14 |
| Recall | 88.50 | 93.81 |
| F1-Score | 89.16 | 93.57 |
| Training Time | 21 min 43 sec | 27 min 95 sec |
| Model Size | 528 MB | 574 MB |

The above table 2 indicates that both VGG16 and VGG19 are effective for soil image classification. VGG19 slightly outperforms than VGG16 in accuracy, precision, Recall, F1-score, training time and model size, VGG16 is more suitable due to its faster inference and smaller size. VGG19 is a better choice for high-accuracy requirements in research and industrial applications. Transfer learning played a crucial role in the high performance of both models, highlighting the importance of pre-trained weights when dealing with limited datasets.

5. Conclusion and Future Scope

This paper presented a comparative analysis of VGG16 and VGG19 Convolutional Neural Network architectures for soil image classification. Both models demonstrated excellent performance, with VGG19 achieving slightly superior accuracy, precision, Recall, F1-score metrics as well as training time and model size. This performance gain attributed to VGG19 is deeper architecture, which enables the extraction of more complex and hierarchical features from soil images. The additional layers in VGG19 allow it to learn finer texture patterns and complex color variations, which are crucial for differentiating between similar soil types. The increased depth of VGG19 comes at the cost of higher computational complexity, longer training times, and larger model size. VGG16, while slightly less accurate, provides faster inference and requires less memory. **VGG19** is achieved a final training accuracy of **96.8%** and validation accuracy of **94.39%**. The validation loss for VGG19 was slightly lower than VGG16, indicating better generalization. The findings suggest that deep learning, especially CNN-based models, effectively classify soil types based on image data.

Future research focus on exploring more efficient and lightweight CNN architectures such as MobileNet, EfficientNet, or ShuffleNet. These models are well-suited for real-time and mobile-based applications, offering a favourable balance between accuracy and computational efficiency. Furthermore, the integration of multi-modal data including hyperspectral images, ASD spectral data, and sensor-based measurements holds promise for enhancing model robustness and enabling the classification of visually similar soil types.

In addition, advanced techniques such as transfer learning, ensemble modelling, and attention-based mechanisms for transformers contribute to further performance improvements. The development of GIS-integrated, mobile-accessible platforms based on these models significantly broaden the practical utility of soil classification systems, making them accessible to end users.

Data Availability

There is one soil image dataset used in this paper. These Images/photographs taken with digital cameras. These Images are in JPEG format. The soil picture dataset represents a variety of soil types such as Black Soil, Laterite Soil, Red Soil, and White Soil. Each image in the collection accompanied by a label or class identifier that indicates the

soil type belongs to which class. This labelling is necessary for supervised machine learning tasks such as classification. Soil images are varied in size and resolution. High-resolution photos that capture tiny features of soil texture, while others may be lower resolution and more suited for broad land categorization. This dataset divided into training (80%) and testing (20%) sets.

Conflict of Interest

The authors have no conflict of interest.

Funding Source

No specific grant received from any funding agency.

Authors' Contributions

Girish D. Chate: Conceptualization, Data Set Preparation, Formal analysis, Methodology, Implementation, Validation and Writing – original draft.

S. S. Bhamare: Conceptualization, Methodology, Validation, Supervision and Writing – original draft.

Acknowledgements

I am grateful to my guide, Dr. Sandip Bhamare for his invaluable guidance throughout this research work. His expertise and unwavering support played a crucial role in the success of this work.

References

- [1] S. A. Khan, et al., "A review of soil classification using machine learning," *Geoderma*, Art. no. 114984, Vol.389, 2021.
- [2] R. McBratney, D. J. Field, and A. B. McBratney, "Future directions of soil science," *Geoderma Regional*, Vol.4, pp.1–5, 2015.
- [3] M. A. Shepherd and M. G. Shepherd, "Modern soil testing and classification," *Soil Use and Management*, Vol.29, No.4, pp.515–525, 2013.
- [4] R. Goswami, A. Saha, and P. Saha, "Soil classification using Convolutional Neural Networks," *Computers and Electronics in Agriculture*, Vol.172, 2020.
- [5] D. Yadav, R. K. Sharma, and N. Kumari, "Deep learning models for soil type classification using image and spectral data," *Environmental Modelling & Software*, Vol.148, 2022.
- [6] A. Krizhevsky, I. Sutskever, and G. E. Hinton, "ImageNet classification with deep convolutional neural networks," in *Proc. NIPS*, pp. 1097–1105, 2012.
- [7] K. Simonyan and A. Zisserman, "Very Deep Convolutional Networks for Large-Scale Image Recognition," *arXiv:1409.1556*, 2014.
- [8] Srivastava P., Shukla A., & Bansal A., A comprehensive review on soil classification using deep learning and computer vision techniques. *Multimedia Tools and Applications*, Vol.80, Issue.3, pp.4667–4694, 2021.
- [9] Deng, Z., Liu, M., & Wang, Y., Hyperspectral image classification using convolutional neural networks and 3D-CNNs. *Journal of Applied Remote Sensing*, Vol.14, Issue.1, pp.014520, 2020.
- [10] Ramesh P., & Suruliandi A., Soil classification using deep convolutional neural networks for Indian soil datasets. *International Journal of Computer Applications*, Vol.178, Issue.21, pp.27–34, 2019.
- [11] Zhang, Y., Li, J., & Chen, Y., Using attention mechanisms for soil classification based on CNNs: A case study in agriculture. *Agricultural Systems*, 190, pp.103092, 2021.

[12] Hossain, M. S., Rahman, M. M., & Goh, A. T. C., Explainable AI for soil classification: Using Grad-CAM to visualize CNN decisions. *Expert Systems with Applications*, 189, pp.116030, 2022.

[13] Nguyen, D. D., Tran, T. P., & Pham, H. D., Federated learning for privacy-preserving soil image classification. *International Journal of Agricultural Science and Technology*, Vol.13, Issue.1, pp.32-43, 2023.

[14] Alam, M. A., Islam, M. R., & Shikder, M. I., Enhancing soil image classification performance with data augmentation and image enhancement techniques. *Computers and Electronics in Agriculture*, 194, 106754, 2022.

[15] P. Goswami, P. P. Roy, and S. Bandyopadhyay, "Soil classification using convolutional neural networks," *J. Soil Sci. Environ. Manage.*, Vol.11, No.4, pp.55-63, 2020.

[16] S. A. Khan, M. Usman, and A. R. Shah, "A review of soil classification using machine learning," *Geoderma*, Vol.389, pp. 114984, 2021.

[17] R. Yadav, D. Gupta, and R. Bhattacharyya, "Hybrid deep learning models for soil fertility classification using image and spectral data," *Environ. Sci. Pollut. Res.*, Vol.29, No.5, pp.6592-6606, 2022.

[18] S. Nandhini and V. Kavitha, "Soil texture classification using deep convolutional neural networks on satellite images," *Remote Sensing Lett.*, Vol.11, No.3, pp.299-308, 2020.

[19] R. Patil, M. K. Choudhury, and H. Joshi, "Real-time soil type prediction using deep learning with a mobile application," *Sensors*, Vol.21, No.9, pp.2995, 2021.

[20] F. Zhao, X. Li, and Y. Zhang, "A comparative study of CNN architectures for soil profile classification using RGB images," *Agric. Informatics*, Vol.3, No.2, pp.113-124, 2022.

[21] Zhang X, Youman NH, King RL. Soil texture classification using wavelet transform and maximum likelihood approach. 7929-7931

[22] Ok S, Hyun K, Youl K (2012) Texture Classification Algorithm Using RGB Characteristics of Soil Images 57, pp.393–397, 2003.

[23] Shenbagavalli R, Ramar K., Classification of soil textures based on Laws features extracted from preprocessing images on sequential and random windows. Bonfring Int J Adv Image Process 1: pp.15–18, 2011.

[24] Sofou A, Evangelopoulos G, Maragos P., Soil image segmentation and texture analysis: a computer vision approach. Geoscience and Remote Sensing Letters Vol.2, Issue.4, pp.394–398, 2005.

[25] Breul P, Gourves R., In field soil characterization: approach based on texture image analysis. Journal of Geotechnical and Geoenvironmental Engineering Vol.132, Issue.1, pp.102–107, 2006.

[26] Shenbagavalli R, Ramar K., Feature extraction of soil images for retrieval based on statistics. Int J Comput Appl 88: pp.8–12, 2014.

[27] Honawad PSK, Chinchali PSS, Pawar PK, Deshpande PP., Soil Classification and Suitable Crop Prediction. pp.25–29, 2017.

[28] Murti GSRK, Satyanarayana KVS. Influence of chemical characteristics in the development of soil colour. Geoderma 5: pp.243–248, 1971.

[29] Chung SO, Cho KH, Cho JW, Jung KY, Yamakawa T. Soil texture classification algorithm using RGB characteristics of soil images. J Fac Agric Kyushu Univ 57: pp.393–397, 2012.

[30] de O. Moraes PA, Souza DM, de M. Carvalho MT, Madari BE, de Oliveira AE, Predicting soil texture using image analysis. Microchem. J. 146: pp.455–463, 2019.

AUTHORS PROFILE

Girish D. Chate earned M. C. A. from Dr. Babasaheb Ambedkar Marathwada University in 2015. He has been a Research Scholar in School of Computer Sciences Kavayitri Bahinabai Chaudhari North Maharashtra University, Jalgaon since 2019. He has 05 years of teaching experience. His research area includes image processing.



Sandip S. Bhamare is working as an Associate Professor in School of Computer Sciences, Kavayitri Bahinabai Chaudhari North Maharashtra University (formerly Known as North Maharashtra University), Jalgaon. His total teaching experience of 18 years and he has published more than 15 papers in reputed peer reviewed national and international journals & conferences. His research area includes Web Mining, Information Retrieval and IOT.

